35th Annual International Conference of the IEEE EMBS
Osaka, Japan, 3 - 7 July, 2013

Dynamics of Hemoglobin States in the Sensorimotor Cortex During Motor Tasks: A Functional Near Infrared Spectroscopy Study

Chia-Feng Lu, Shin Teng, and Yu-Te Wu

Abstract— **In this study, we used functional near infrared spectroscopy (fNIRS) imaging to investigate the independent levels of oxygenated, deoxygenated, and total hemoglobin (oxy-Hb, deoxy-Hb, and total-Hb, respectively) at the sensorimotor cortex during hand-grasping motor tasks. Our results showed that the activation of contralateral primary motor cortex (M1) exhibited increased oxy-Hb and reduced dexoy-Hb after hand grasping began. Meanwhile, the contralateral primary somatosensory cortex (S1) was deactivated with reductions of both oxy-Hb and deoxy-Hb concentration. The Hb circulation patterns indicated that the hand grasping demanded rapid and sufficient O_2 supply at contralateral M1, which was achieved by the local vasodilation. The contralateral S1 presented decreased total-Hb via the mechanism of vasoconstriction, and maintained the local oxygenation level in a relatively stable state (mostly with O_2 debt) to compensate the blood demanding at nearby M1. This study presented that fNIRS data can efficiently differentiate the activation of M1 from the deactivation of S1 during motor tasks, which can provide full interpretations of hemodynamic response to the neuronal activation in comparison with the Blood Oxygenation Level Dependent signal of functional magnetic resonance imaging.**

I. Introduction

Functional near infrared spectroscopy (fNIRS) is an optical neuroimaging method that monitors the activation of cortical neurons by hemodynamic response on the basis of the tight coupling between neuronal activation and vascular response. The measures of fNIRS can be used to track temporal variations of the hemoglobin (Hb) state as a marker for neuronal activation. Unlike the Blood Oxygenation Level Dependent (BOLD) signal of functional magnetic resonance imaging (fMRI), which principally depends on the level of deoxy-hemoglobin (deoxy-Hb) [1-2], the fNIRS can independently measure the concentrations of oxy-hemoglobin (oxy-Hb) and deoxy-Hb. Therefore, fNIRS data allow for a richer characterization of the underlying neuronal activation from the perspective of the blood oxygenation than the BOLD signal of fMRI data.

Previous studies defined 6 combinatorial Hb states based on the levels of 3 hemoglobin components, i.e. oxy-Hb, deoxy-Hb, and total hemoglobin (total-Hb), to describe the hemodynamic response to neuronal activation [3-4]. In this study, we acquired both the fMRI and fNIRS data during the hand grasping from ten healthy participants to investigate whether these two datasets can identify compatible activation regions, and whether the independent measurements of oxy-Hb and deoxy-Hb from fNIRS data can provide further physiological information of the underlying mechanism of tissue-vascular coupling.

II. Material and Method

A. Participants

This study received prior approval from the local Institutional Review Board. Ten right-handed, healthy adults (5 males/ 5 females), with a mean age of 22.7 years old (range: 19–27 years) were recruited. Each participant provided written informed consent before participating in the study. Exclusionary criteria were a history of neurological disease, psychiatric disorders, or drug use disorders.

B. Data collection for fNIRS

A multi-channel, continuous wave, near infrared tomographic imager (DYNOT Imaging System, Model 932, NIRx Medical Technologies LLC, Glen Head, NY 11545) was used to simultaneously acquire the dual-wavelength (760 and 830 nm) signals using a 5× 6 array of 5-mm diameter optical fibers that covered the surface area of left sensorimotor cortex (Fig. 1). The distance between adjacent optodes was about 2 to 3 cm. Illuminating near infrared light was conducted from imager to the participant's head via 9 bifurcated optical fibers, and detected photons were received by the same 9 bifurcated optical fibers and other 21 detector fibers, that is, overall 9 light sources (white circles in Fig. 1a) and 30 detectors (both white and gray circles in Fig. 1a) were employed in this study. Using a fast optical switch, the 5× 6 optical array can be scanned at a framing rate of 7.42 Hz. To facilitate good contact with the scalp, the optodes were spring loaded and housed on an open scaffolding helmet (Fig. 1b). All the optical fibers were supported by a multi-axis articulating arm for off-loading the weight of fibers from participant's head. Participants were seated in a comfortable armchair and stared at a monitor placed approximately 90 cm away at eye level for the visual instruction of motor tasks.

This research was supported in part by the National Science Council (NSC100-2221-E-010-009, NSC101-2221-E-010-004-MY2) and Brain Research Center, National Yang-Ming University and a grant from Ministry of Education, Aim for the Top University Plan.

Chia-Feng Lu is with the Dept. of Biomedical Imaging and Radiological Sciences, Brain Research Center, National Yang-Ming University, Taipei, Taiwan, ROC (e-mail: alvin4016@ yahoo.com.tw).

Shin Teng is with the Dept. of Biomedical Imaging and Radiological Sciences, National Yang-Ming University, Taipei, Taiwan, ROC (e-mail: iamtengshin@ yahoo.com.tw).

Yu-Te Wu is with the Dept. of Biomedical Imaging and Radiological Sciences, Brain Research Center, National Yang-Ming University, Taipei, Taiwan, ROC (corresponding author, phone: +886228267169; fax: +886228201095;e-mail: ytwu@ym.edu.tw).

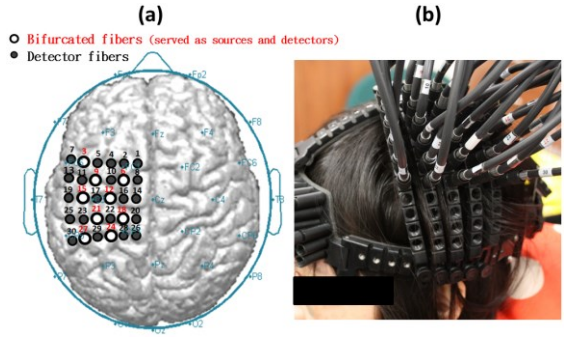

Figure 1. (a) Top view of the optical fiber arrangement covering the surface region of left sensorimotor cortex. (b) The installation of 30 optical fibers on an open scaffolding helmet.

C. Image acquisition for fMRI

To compare with fNIRS data, we also acquired anatomical MRI and fMRI images for each participant using a 3T MR system (MAGNETOM Trio, A Tim System, Siemens, Germany) after the fNIRS data collection. The T1-weighted images were acquired using a 3D fast spoiled gradient echo pulse sequence (TR = 2530 ms, TE = 3.03 ms, flip angle = 7°, FOV = 224× 256× 192 mm^3, matrix size = 224× 256× 192). The fMRI data were acquired by a multi-slice gradient echo (TR = 2000 ms, TE = 20 ms, flip angle = 90°, matrix size = 64× 64, FOV = 220× 220 mm^2, slice thickness = 3.4 mm). The slices covered the entire cerebral and cerebellar cortices. A mirror was attached to the head coil of the MR scanner for allowing participants can be informed via a video screen for the subsequent motor tasks.

D. Experimental design

We employed a block design with two conditions, i.e. the grasping condition and resting condition. The experiment was begun with a long resting condition (60 s) followed by alternately grasping and resting conditions (block length 20 s) (Fig. 2). The resting condition was given by a white cross fixed in the center of screen, and the grasping condition was instructed by a red cross with 1-Hz blinking rate in the screen. In the grasping conditions, participants were asked to perform repeated whole-hand grasping with right hands following the blinking rate of red cross in the screen. In the resting condition, participants were asked to relax their hands until next grasping condition. Fig. 2 displays the block design (the blue curve) and the anticipated hemodynamics, which is obtained from the convolution of the block design wave with the hemodynamic response function (the black dotted line).

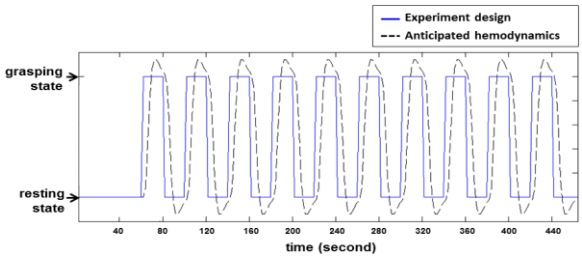

Figure 2. The block design of the conducted motor task.

The overall time length of motor experiment is 460 s, and therefore 230 image volumes for fMRI and about 3418 frames for fNIRS data were acquired.

E. Data analysis for fNIRS

The fNIRS data were pre-processed using the Near-infrared Analysis, Visualization and Imaging (NAVI) software package (NIRx Medical Technologies LLC, Glen Head, NY 11545) [5]. The raw data for both illumination wavelengths were low-pass filtered with 0.5 Hz cutoff to exclude the cardiac frequency, and the channels with a noise threshold of coefficient-of-variation (CV) larger than 20% were discarded. Each time series of detected signal was divided by the time series of the signal from the bifurcated fibers to correct the variations in laser power and coupling efficiency of the optical switch [4].

The tomography of the absorption coefficient (μ_a) for both 760- and 830-nm wavelengths were computed using the normalized difference method, applied to a finite element mesh computed from the T1-weighted image volume for a healthy participant [6]. The concentration maps of oxy-Hb and deoxy-Hb were computed by solving linear equations of dual-wavelength μ_a values for each image voxel [7]. The Hb maps were then spatially normalized to the T1 template image with voxel size 2× 2× 2 mm^3 by applying the transformation matrix of the corresponding anatomical T1-weighted images to the T1 template. The flowchart of fNIRS image processing is given in Fig. 3a.

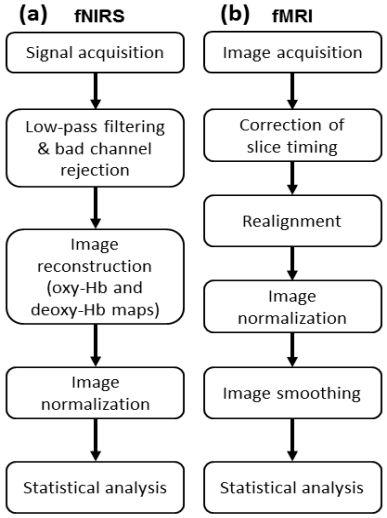

Figure 3. The flowcharts of image processing for (a) fNIRS and (b) fMRI data.

F. Data analysis for fMRI

The pre-processing of fMRI data was conducted using statistical parametric mapping software (SPM8, http://www.fil.ion.ucl.ac.uk/spm/) [8]. The image volumes were corrected for acquisition time delay among different slices, followed by the realignment for head-motion correction (a 6-parameter affine transformation). All the corrected fMRI images were registered to the corresponding anatomical T1-weighted images to achieve spatial normalization to the T1 template image with voxel size

$2 \times 2 \times 2$ mm^3. Finally, spatial smoothing with a 6-mm full width at half maximum (FWHM) Gaussian kernel was applied to the normalized images. The flowchart of fNIRS image processing is presented in Fig. 3b.

G. Statistical analysis using general linear model

General linear model (GLM) was used to investigate the correlation between the anticipated hemodynamics (the black dotted line in Fig. 2) and time series of BOLD/oxy-Hb/deoxy-Hb at each voxel [8]. The voxel with significant activation (positive correlation) or deactivation (negative correlation) was identified if its corresponding p-value of t-statistics was smaller than 0.05 under the correction of false discovery rate (FDR).

III. Results and Discussion

A. The motor activations in fMRI data

Fig. 4 presents the activation regions obtained from fMRI data during the right-hand grasping task for a representative participant. The most significantly activated motor region (colored by light yellow) was in the contralateral primary motor cortex (M1) and part of primary somatosensory cortex (S1). A minor activation of the supplementary motor area (SMA) and ipsilateral M1 was also observed.

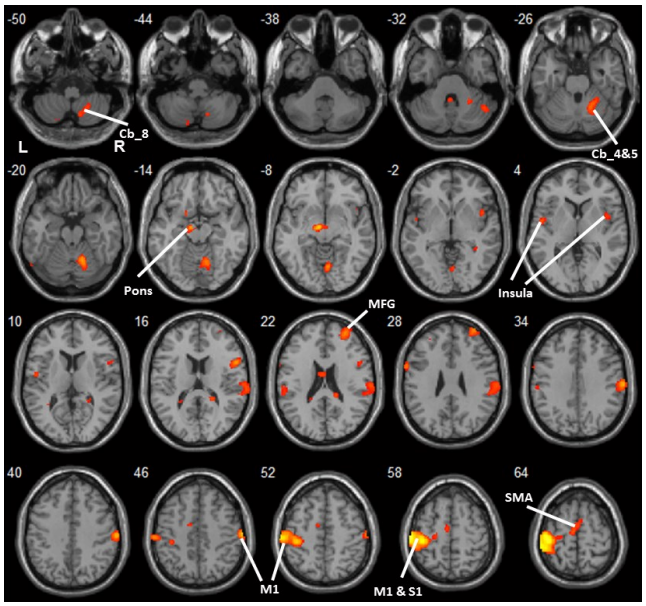

Figure 4. The activation regions in fMRI data. M1: primary motor cortex; S1: primary somatosensory cortex; SMA: supplementary motor area; MFG: middle frontal gyrus; Cb_4&5: cerebellar lobule IV & V; Cb_8: cerebellar lobule VIII.

These activated regions associated with hand movement were consistent with the previous study [9]. Other motor-related activations were located at bilateral insulae, contralateral pons, and ipsilateral cerebellar regions (Fig. 4).

Fig. 5 displays the voxel with the largest response to the motor task and the corresponding BOLD signal of block average.

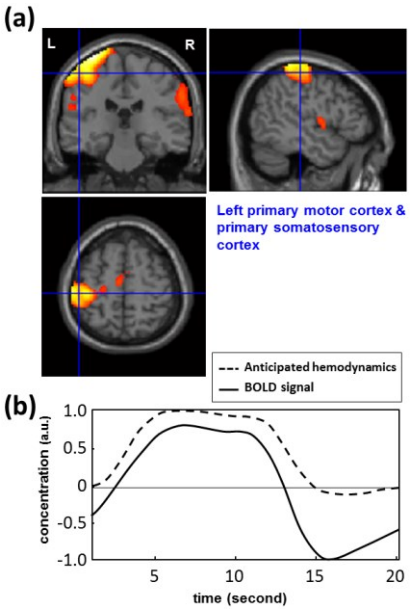

Figure 5. (a) The voxel with the largest response and (b) the corresponding BOLD signal of block average.

B. Six combinatorial Hb states

Six combinatorial Hb states were defined in the previous studies to describe the hemodynamic response to neuronal activation [3-4]. In the following sections, we discuss the physiological correlates of Hb states based on these 6 conditions (Table I).

TABLE I. Definitions of the Combinatroial Hb States

	State 1	State 2	State 3	State 4	State 5	State 6
Oxy-Hb	−	−	−	+	+	+
Deoxy-Hb	−	+	+	+	−	−
Total-Hb*	−	−	+	+	+	−
	Balanced	Uncomp. O_2 debt	Comp. O_2 debt	Balanced	Uncomp. O_2 excess	Comp. O_2 excess

*Total-Hb is simply calculated by the sum of oxy-Hb and deoxy-Hb.

Uncomp.: Uncompensated; Comp.: Compensated.

C. The activations of M1 in fNIRS data

For the same representative participant, the motor-related activations were primarily located at the contralateral M1 (light yellow in Fig. 6a). Once the hand grasping began, the local oxy-Hb increased with reductions of deoxy-Hb until the maximal concentration of oxy-Hb was reached at about 6 s after the beginning of grasping (Fig. 6b).

The circulation of Hb states was initiated from the State 3 (O_2 debt) to State 5 & 6 (O_2 excess) and then back to State 2 & 3 (O_2 debt) with short intervals of balanced State 1 & 4 (Fig. 6c). This result indicated that the activation of M1 during the hand grasping demanded rapid and sufficient O_2 supply, which was achieved by the local vasodilation.

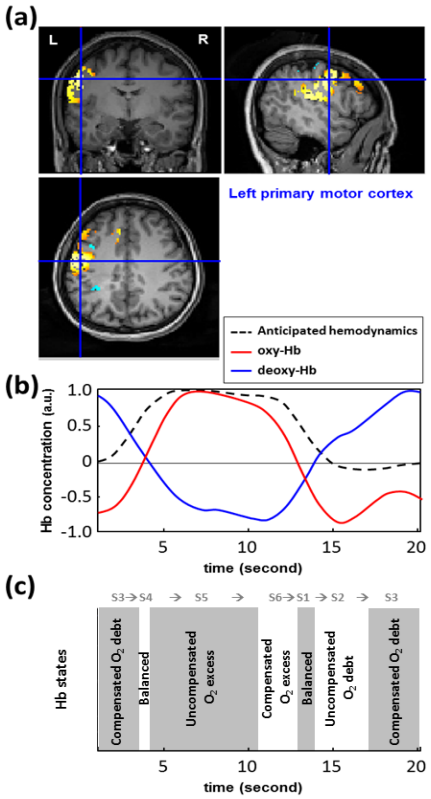

Figure 6. (a) The voxel in M1 with the largest activation of oxy-Hb and (b) the corresponding oxy-Hb and deoxy-Hb signals of block average. (c) The transition of Hb states during motor tasks.

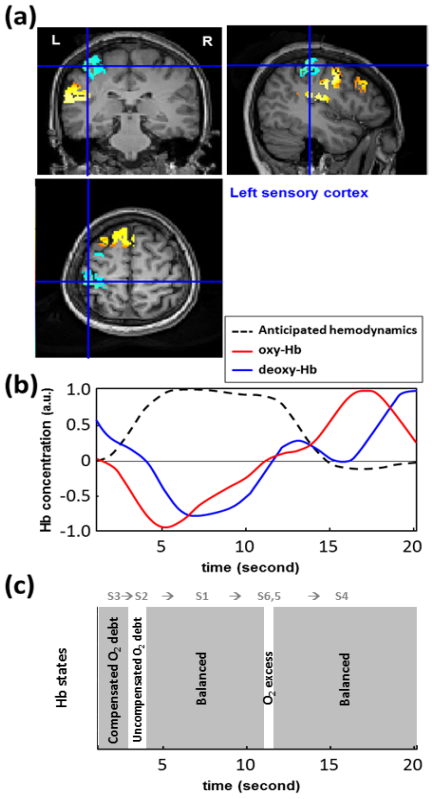

Figure 7. (a) The voxel in S1 with the largest deactivation of oxy-Hb and (b) the corresponding oxy-Hb and deoxy-Hb signals of block average. (c) The transition of Hb states during motor tasks.

D. The deactivations of S1 in fNIRS data

The motor-related deactivations were primarily located at the contralateral S1 (light blue in Fig. 7a). Unlike the hemodynamic responses in the contralateral M1, both the oxy-Hb and deoxy-Hb at the S1 were reduced dramatically during the hand grasping (Fig. 7b), that is, the total-Hb was decreased at the S1 to compensate the demanding of blood supply for the nearby activated M1.

The patterns of Hb circulation at S1 were also different from that at M1. The balanced states (State 1 and 4) occupied most periods of hand grasping (Fig. 7c), leading to a relatively stable Hb state (mostly with O_2 debt) in the deactivated S1 region.

IV. Conclusion

In this study, we presented that the fNIRS data were able to provide a full interpretation of hemodynamic dynamics. Since the BOLD signal used in fMRI studies was principally sensitive to the level of the deoxy-Hb, it was theoretically unable to differentiate the activation or deactivation of oxy-Hb between M1 and S1 regions during motor tasks. Besides, BOLD signal cannot be used to assess the concentration of total-Hb for assessing the underlying mechanism of local vasodilation or vasoconstriction. The applications of fNIRS imaging can be further used in the detection of movement disorders.

References

[1] S. Ogawa, T. M. Lee, A. R. Kay, D. W. Tank, "Brain magnetic resonance imaging with contrast dependent on blood oxygenation," *Proc. Natl. Acad. Sci.*, vol. 87, pp. 9868-9872, 1990.

[2] A. Kleinschmidt, H. Obrig, M. Requardt, K. D. Merboldt, U. Dirnagl, A. Villringer, J. Frahm, "Simultaneous recording of cerebral blood oxygenation changes during human brain activation by magnetic resonance imaging and near-infrared spectroscopy," *Journal of Cerebral Blood Flow & Metabolism*, vol. 16, pp. 817-826, 1996.

[3] G. R. Wylie, H. L. Graber, G. T. Voelbel, A. D. Kohl, J. DeLuca, Y. Pei, Y. Xu, R. L. Barbour, "Using co-variations in the Hb signal to detect visual activation: A near infrared spectroscopic imaging study," *NeuroImage*, vol. 47, pp. 473-481, 2009.

[4] R. L, Barbour, Y. Pei, M. Farber, H. L. Graber, T. Xu, D. Sreedharan, "Functional imaging of autoregulation," *The Organization for Human Brain Mapping*, Chicago, IL, 2007.

[5] Y. Pei, Z. Wang, Y. Xu, H. L. Graber, R. Monteriro, R. L. Barbour, "NAVI: a problem solving environment (PSE) for NIRS data analysis," *Fifth Inter-Institute Workshop on Optical Diagnostic Imaging from Bench to Bedside. Bethesda*, MD, 2006.

[6] A. Y. Bluestone, G. Abdoulaev, C. H. Schmitz, R. L. Barbout, A. H. Hielscher, "Three-dimensional optical tomography of hemodynamics in the human head," *Optics Express*, vol. 9, issue 6, pp. 272-286, 2001.

[7] J. Choi, M. Wolf, V. Toronov, U. Wolf, C. Polzonetti, D. Hueber, L. P. Safonova, R. Gupta, A. Michalos, W. Mantulin, E. Gratton, "Noninvasive determination of the optical properties of adult brain: near-infrared spectroscopy approach," *J. Biomed. Opt.*, vol. 9, issue 1, pp. 221-229, 2004.

[8] K. J. Friston, J. T. Ashburner, S. J. Kiebel, T. E. Nichols, W. D. Penny, "Statistical Parametric Mapping: The Analysis of Functional Brain Images," 1st ed, London: *Academic Press*, 2007.

[9] C. Grefkes, S. B. Eickhoff, D. A. Nowak, M. Dafotakis, G. R. Fink, "Dynamic intra- and interhemispheric interactions during unilateral and bilateral hand movements assessed with fMRI and DCM," *NeuroImage*, vol. 41, pp. 1382-1394, 2008.